CHAPTER 3

CHARACTERIZATION OF INDUSTRIAL SOLID WASTE AS A MOLD MATERIAL

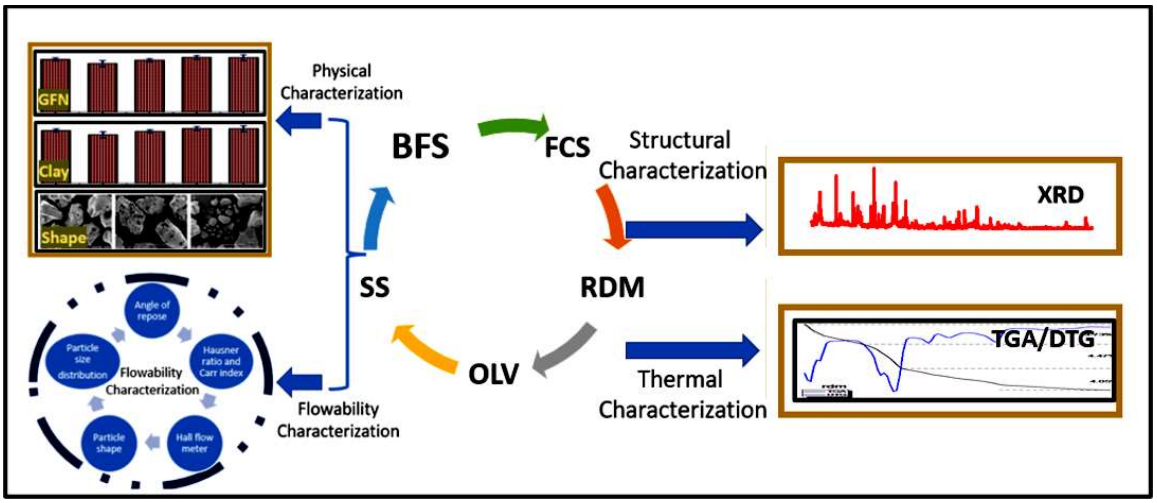

3.1 INTRODUCTION

The present investigation has an intention to utilize a large amount of waste generated from industries, as a mold material for foundry practice. Since the idea is new, hence the characterization of such waste material may affect the structural property relationship for the alloy(s) produced in this way. Hence first, a separate study has been made in this direction. This chapter describes the physical, structural, thermal, and flowability characterization of industrial solid waste as well as conventional mold material and the details of characterization techniques involved for the present investigation such as EPMA, flowability behaviour, sieve analysis, clay content, scanning electron microscopy, TGA and X-ray diffraction and results of flowing characterization with the comparison of conventional mold material.

3.2 CHARACTERIZATION

3.2.1 Chemical analysis

A non-destructive elemental analysis approach called Electron Probe Micro Analyzer (EPMA) analyses micron-sized volumes at the surface of materials in both qualitative and quantitative fashion. For EPMA to function, a sample must first be subjected to a concentrated electron beam with an energy of typically between 5 and 30 keV, and then the X-ray photons that the various elemental species emitted as a result must be collected. When WDS (Wavelength Dispersive Spectroscopy) spectra are taken, it is simple to determine the sample composition can be easily identified by recording WDS spectra. Utilizing a LEICA-EM ACE200 apparatus is the Electron Probe Micro Analyzer (EPMA) CAMECA SX Five instrument. The CAMECA SX Five instrument was run by SX Five Software using a LaB6 source in the electron cannon to generate an electron beam at a voltage of 15 kV and a current of 40 A.

3.2.2 Xray- diffraction (XRD)

The basis of XRD is Bragg's equation, which may be explained in terms of the reflection of an incidence of a collimated X-ray beam on a crystal plane of the sample. The X-rays that are scattered interfere with one another in a useful way. The Bragg's Law can be used to examine this interference and examine various properties of the materials. To ascertain the phases contained in the materials, an analytical X-ray diffractometer with Cu ka radiation, 40 kV accelerating voltage, and 40 mA current is used. The data were recorded at a scanning rate of 5° per minute between 10° - 90°.

3.2.3 Thermogravimetric analysis (TGA)

It is a method of thermal analysis. The thermodynamic analysis relies on the dynamic relationship between temperature and a change in a physical property, like a change in mass or enthalpy, among others. The mass of the substance is continuously measured by TGA as the temperature increases linearly. A method for measuring thermal stability as a function of temperature with a constant heating rate is called thermogravimetric analysis (TGA). The endothermic or exothermic peak indicates when the sample has undergone physical and chemical changes during heating. TGA was used to calculate the weight change while the material was heated to 1000°C.

3.2.4 Clay and moisture content

IS 1918-1966 standard was used for the analysis of clay and moisture content. To perform the clay test, 50 grams of dried sample was taken and mixed into a solution containing 475 cc of distilled water and 25 cc of 3% NaOH solution. After that, it was agitated with a mechanical stirrer for 5 minutes and then diluted with water to a height of 6 inches and let settle for 10 minutes. Now 5-inch water was siphoned and again diluted to 6 inches and let settle for 5 minutes. These steps were repeated enough times (5 times in

general) so that after settling for 5 minutes the water was clean. Now the water from the beaker was taken out and the remaining sand grains were collected, dried, and then weighed to find the weight loss. The difference in the weight loss estimates the percentage of clay present in the sample using equation (3.1).

$$\%clay\ content = \frac{w_1 - w_2}{w_1} \times 100 \quad (3.1)$$

Where;

w_1= weight of the dried sample taken for the test

w_2= weight of the dried sample free from clay

Initially, 100 gm of a sample was taken and dried in a uniformly heated oven between 105℃-110℃ for about one hour, then cool to room temperature and weighed it. Repeat the process of drying and cooling till the constant weight of the sample attain after cooling, then moisture % was calculated using equation (3.2).

$$Moisture\ \% = \frac{A}{B} \times 100 \quad (3.2)$$

Where;

A= loss of weight of the sample after drying.

B= weight of the initial sample.

3.2.5 Sieve analysis

Particle size distribution (PSD) analysis (grain fineness number) of the materials was carried out through sieve analysis following the AFS standard (AFS 1105-12) procedure. Initially, materials were dried in the oven at 110℃ for 1h and then cooled to room temperature. Each 50-gm sample was sieved using a different series of sieves as per IS standards. The test was conducted on a sieve shaker machine for 15 min, which vibrates

and hammers mechanically. The retained sample on each sieve was weighed using a weighing machine and the grain fineness number was obtained using equation 3.3 whereas figure 3.1 shows the particle size distribution, which depicts the mass percentage of specific size or the passing % of specific size. The morphology of particles of different materials was identified by Scanning electron microscopy (SEM).

The grain fineness number (GFN) is expressed as:

$$GFN = \frac{\sum M_n f_n}{\sum f_n} \tag{3.3}$$

Where;

Mn = multiplying factor of the nth sieve

fn = percentage of sand remains on the nth sieve

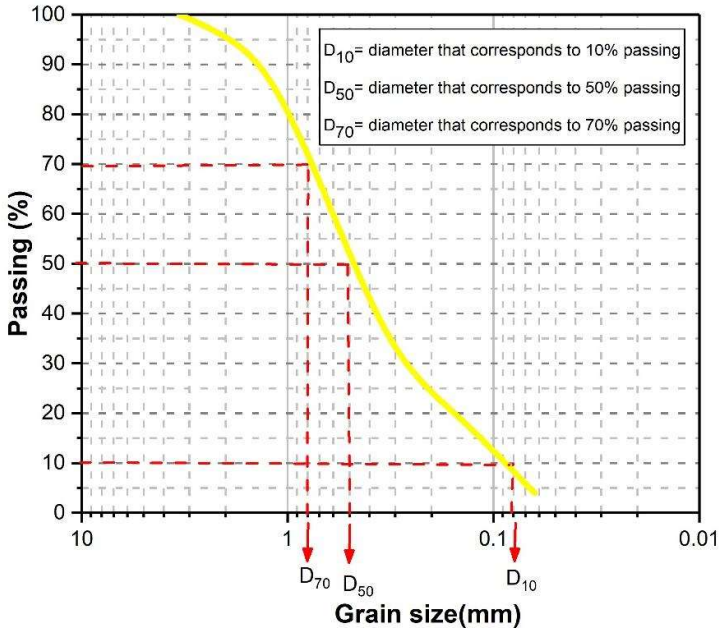

Figure 3.1: Particle size distribution

3.2.6 Flowability behaviour

To know the flowability behaviour of powder or bulk material, the characterization techniques may be static and dynamic based on the condition of the powder. These techniques include angle of repose (static or dynamic) [168,169], Hausner ratio, and Carr index[170] as listed in table 3.1.

Table 3.1: Flow behaviour [41] [37]

Flow character	Compressibility (Carr index)	Angle of repose	Hausner ratio
Very free-flowing	≤ 10	<30°	1.00-1.11
Free-flowing	11-15	30°- 38°	1.12-1.18
Fair	16-20	38°- 45°	1.19-1.25
Passable	21-25	45° - 55°	1.26-1.34
Poor	26-31	>55°	1.35-1.45
Very poor	32-37	<30°	1.46-1.59
Very, very poor	≥ 38	--	≥ 1.60

i. *The angle of repose (AOR)*

The angle that the surface of the sand pile makes with the horizontal is known as the angle of repose. The static AOR was analyzed as per ASTMC144. In the beginning, the gap between the conical glass and lid was fixed and outlet of the funnel was kept close with a stopper and the sample was filled in the funnel. As soon as the stopper was removed, the sand starts falling due to gravity. To maintain a rate of discharge and standard height of the pile sample was continuously fed to the funnel. Due to the constant height, the diameter was measured by drawing a circle through the base of the sand pile, and the angle of repose was measured as per equation 3.4 [171–173]. The reported value is the average of three repeated experiments and is compared with table 3.1. Figure 3.2 shows the setup of the AOR.

$$tan\phi = \frac{h}{(D-d)/2} \quad (3.4)$$

Where h= height of granules pile,

D = diameter of granules pile and d (internal diameter of the funnel) = 5mm.

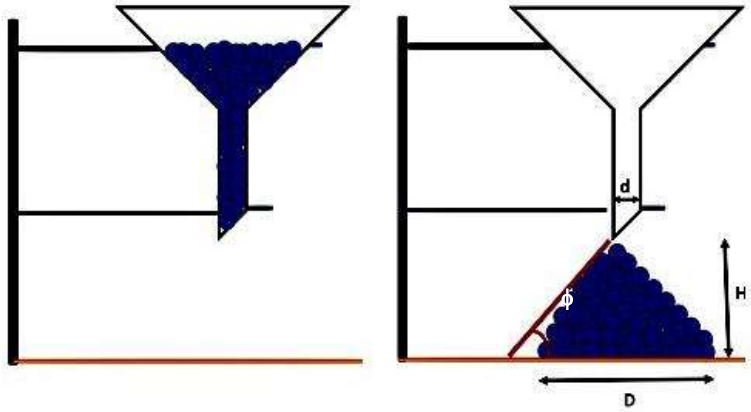

Figure 3.2: Setup of the angle of repose

ii. *Hall flow meter test*

In this test, the time required for powder flow through the Hall funnel was noted as per standard ISO4490. A known quantity of samples was put in the funnel with the orifice closed. After opening the orifice, powder starts falling into the measuring tube due to gravity. The volume or mass of the powder is measured as per density variation. If the density variation is less mass of the sample is kept fixed otherwise the volume of the powder sample is fixed. But in the mold-making process, a cavity of the mold box is filled with the volume of the sand rather than mass. Therefore, the time required to flow 30 ml of mold material through the glass funnel was measured. Three times each test was repeated and average values were reported.

iii. *Hausner ratio and Carr index*

The ratio of tapered density to bulk density is known as the Hausner ratio (HR) whereas, the ratio of change in tapper density and bulk density to tapped density is known as the Carr index (CI) as per equations 3.5 and 3.6. The interaction between a particle's shape, size,

surface properties, etc is the important factor that decides the bulk density of a material. In this test, 100 ml of sample was filled in a cylindrical tube with a funnel. The cylinder was tapped by a sieve shaker machine for one minute, and then the final volume of the sample was measured. Initial and final mass was kept constant only the volume of the sample was changed and hence Hausner ratio may also be defined as the ratio of bulk volume to tapered volume of the sample. The flowability characteristics behaviour with respect to the Hausner ratio are tabulated in table 3.1 and indicates that the lower the value of the ratio better the flowability [174,175].

$$\mathrm{HR} = \frac{\text{Tapped density}}{\text{Bulk density}} = \frac{\text{Bulk volume}}{\text{Tapped volume}} \tag{3.5}$$

$$\mathrm{CI} = \frac{\text{Tapped density} - \text{Bulk density}}{\text{Tapped density}} \times 100 \tag{3.6}$$

3.3 RESULT AND DISCUSSION

3.3.1 Chemical analysis

The chemical analysis of materials is listed in table 3.2, which states that SiO_2 is one of the major common constituents present in all the materials, which play a vital role to decides whether this solid waste can be an alternative to conventional mold material and physical appearance of as received solid waste and sand are shown in figure 3.3.

Table 3.2: Chemical composition of mold materials

Materials	SiO_2	MgO	CaO	TiO_2	FeO	Al_2O_3	Fe_2O_3	Na_2O	Cr_2O_3
SS	99.47	-	0.001	0.059	0.04	-	-	-	-
BS	32.57	10.78	34.62	1.078	0.29	18.92	-	0.2105	0.0658
OL	40.21	50.92	0.007	0.048	8.00	-	-	-	0.0070
RM	7.45	-	-	13.68	-	15.02	40.42	5.02	-
FS	26.03	23.43	5.03	-	-	25.37	2.89	-	11.85

3.3.2 Physical appearance

Figure 3.3: Material used for mold preparation (a) blast furnace slag (b) ferrochrome slag (c) red mud (d) olivine sand (e) silica sand

3.3.3 X-Ray Diffraction (XRD)

To identify the minerals, present in the raw materials, an X-ray diffraction (XRD) study of blast furnace slag, ferrochrome, red mud, and silica sand was carried out. Calcite ($CaCO_3$), Quartz (SiO_2), MgO_2, Al_2O_3, and C_2CaMgO_6 are the minerals found in blast furnace slag. The composition of the iron ore, flux stone, coal, or coke, operating temperature, and quantity of basicity utilized in the furnace operation all affect the minerals contained in the blast furnace slag. Calcite ($CaCO_3$), Fosterite (Mg_2O_4Si), SiO_2, and Spinel (Al_2MgO_4) are the minerals found in ferro chrome. The type of ore, flux, oxygen partial pressure, reduction temperature, and time spent in a high-temperature zone of the furnace all affect the ferrochrome slag's composition. Hematite (Fe_2O_4), TiO_2, Al_2O_3, SiO_2, and CaO are all present in red mud. The location of the bauxite ore, the type of processing, and the method of storage all affect the red mud's chemical makeup. Sand is primarily made of quartz (SiO_2) and contains calcite ($CaCO_3$). According to figure 3.4, quartz (SiO_2) is the common constituent phase of all raw materials.

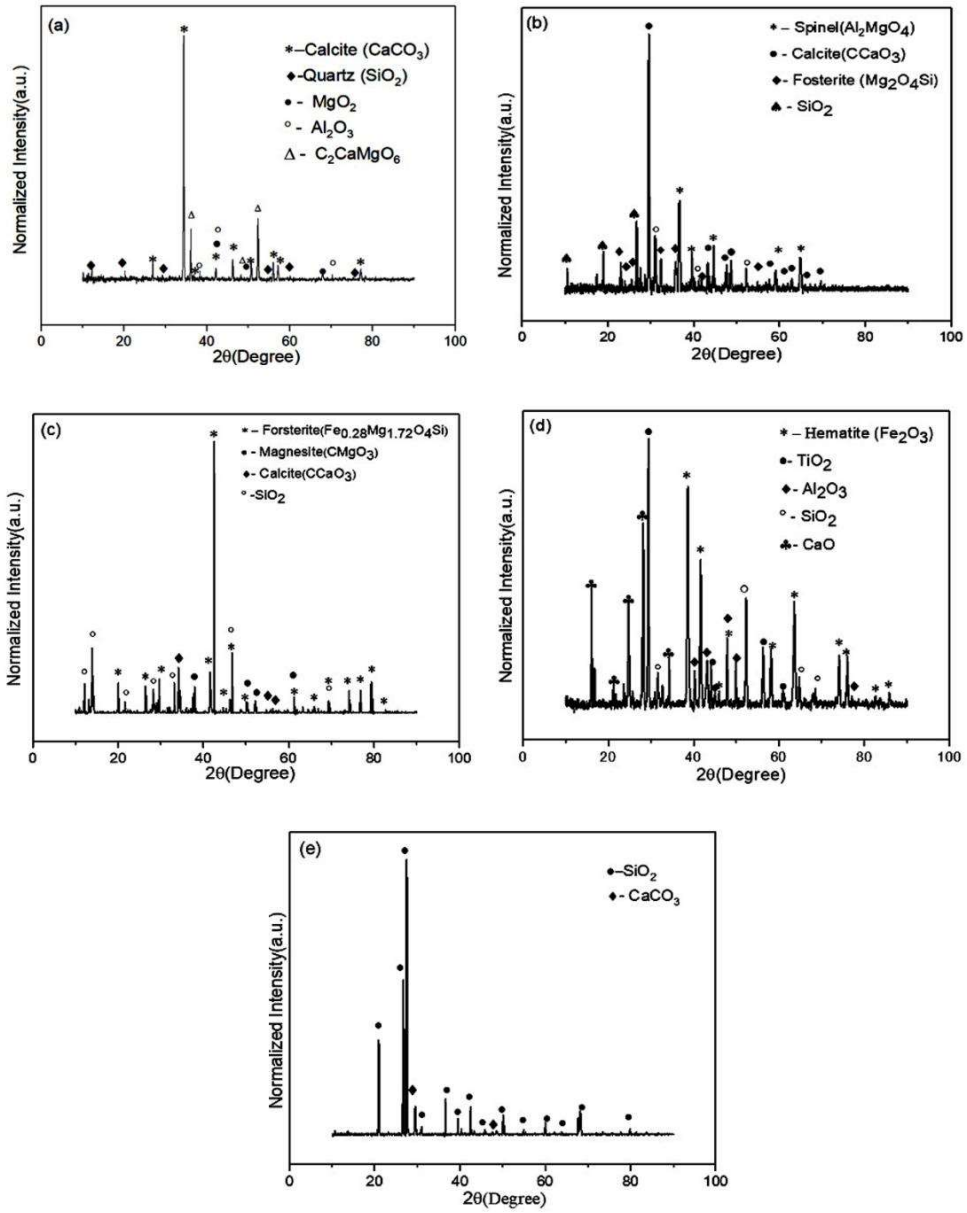

Figure 3.4: XRD pattern of (a) blast furnace slag (b) ferrochrome slag (c) olivine sand (d) red mud (e) silica sand

3.3.4 Thermogravimetric analysis (TGA)

A method for measuring thermal stability as a function of temperature with a constant heating rate is called thermogravimetric analysis (TGA). The endothermic or exothermic peak indicates when the sample has undergone physical and chemical changes during heating. TGA was used to calculate the weight change while the material was heated to

1000°C. Figure 3.5 displays the thermogravimetric analysis (TGA) and derivative thermogravimetric analysis (DTG) results for blast furnace slag, ferrochrome slag, olivine sand, red mud, and silica sand mold. According to figure 3.5, a weight reduction of 4.4%, 3.5%, 3.1%, 10.07%, and 12.25% for blast furnace slag, ferrochrome slag, silica sand, olivine sand, and red mud, respectively, was seen in the range of RT-1000°C at 10°C/min. At low temperatures, the weight loss was caused by moisture that was present on the surface of these materials evaporating, whereas, at high temperatures, the weight loss was caused as a result of the phase transformation. Figure 3.5 shows that the weight reduction for blast furnace slag, ferrochrome slag, silica sand, and olivine sand over 750°C was negligible.

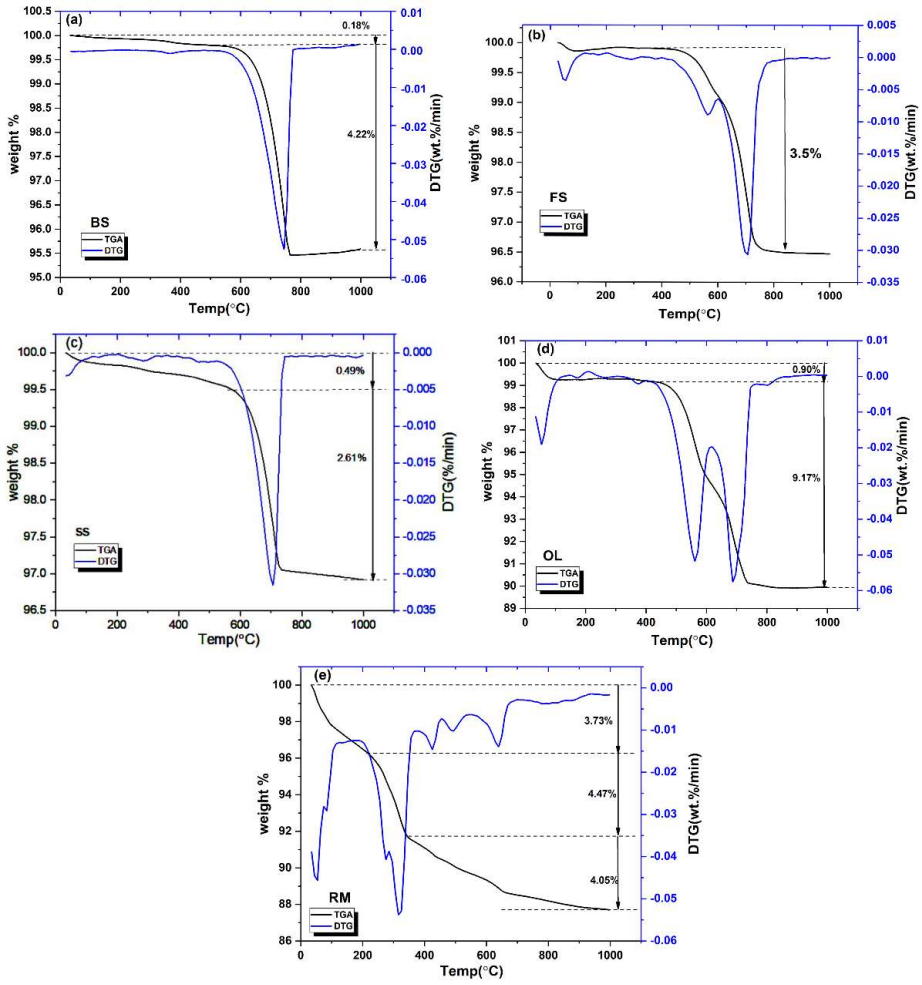

Figure 3.5:TGA plot of (a) blast furnace slag (b) ferrochrome slag (c) silica sand (d) olivine sand (e) red mud

3.3.5 Particle Shape and particle size distribution

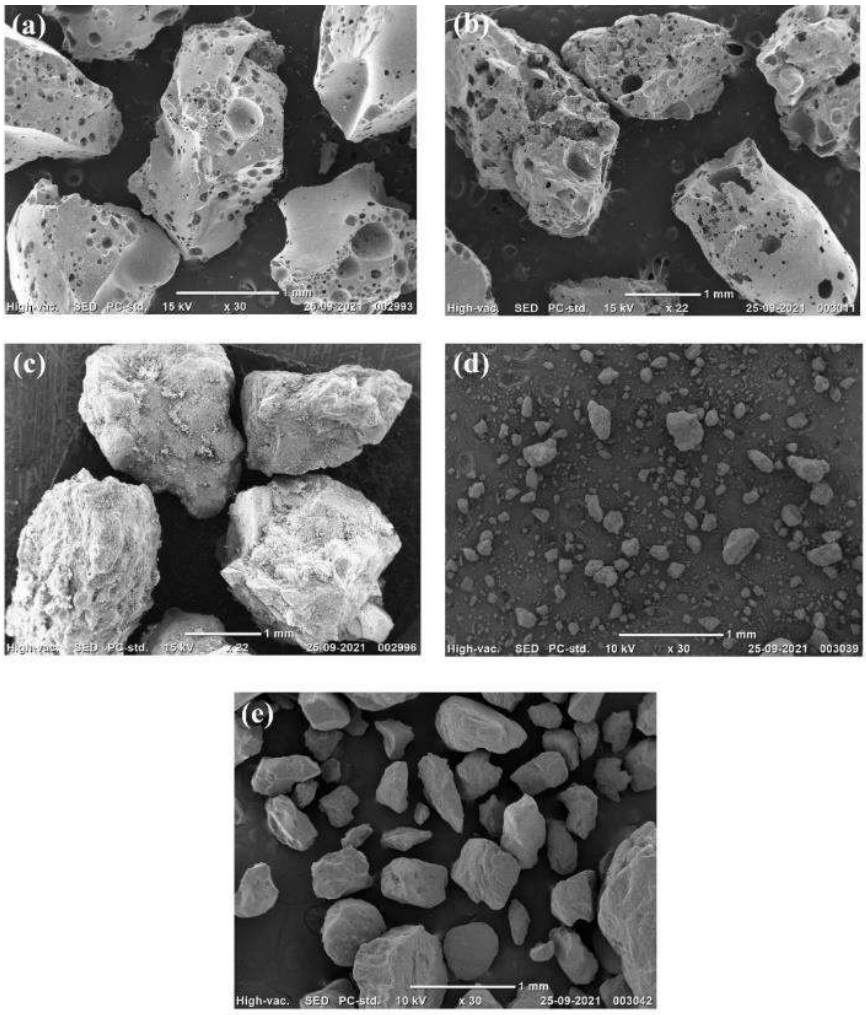

Figure 3.6: SEM images showing particle shape (a) blast furnace slag (b) ferrochrome slag (c) olivine sand (d) red mud (e) silica sand

The SEM image of particles were shown in figure 3.6. Some particles exhibit an irregular shape and globular shape (figure 3.6). The size of blast furnace slag, ferrochrome slag, and olivine sand particles are having larger grains as compared to sand and red mud particles. High sensitivity circularity (HSC) is one of the shape factor parameters defined in equation 3.7, which estimates the circularity of the particle shape as tabulated in table 3.3. Particles having an HSC value of 1 represent a perfect circle whereas, one having an HSC value less than 1 resembles an irregular shape [176]. RM particles are circular (HSC

value 1) whereas BS, OL, and SS particles are having approximately the same shape as shown in table 3.3 due to HSC value in the range of 0.702 - 0.744. Hence, safely it can be assumed that interparticle interaction behaviour in BS, OL, and SS material will be the same.

$$HSC = \frac{4\pi \times area}{(perimeter)^2} \tag{3.7}$$

From the results of sieve analysis, the D50 of BS, FS, OL, RM, and SS was observed to be 1 mm, 1 mm, 2.34 mm, 0.212 mm, and 0.3 mm as shown in figure 3.7. From figure 3.6, size of the 50% of aggregates of BS of 1mm - 0.1 mm and FS of 1mm - 0.1 mm are much close to the range of silica sand grain size, whereas 20% of OL aggregates have a range of 1mm - 0.1mm and rest of 80% are above 1mm. For the RM, 90% are in the range of 1mm - 0.1 mm. This states that the BS and FS show similar behaviour to silica sand with respect size of the particle. The grain fineness number (GFN) of RM was observed high whereas OL has low GFN which means that RM particles are finer as compared with OL particles as shown in table 3.3.

Table 3.3: High sensitivity circularity (HSC) and GFN of materials

Materials	Area (mm^2)	Perimeter (mm)	HSC	GFN
BS	6.00 ± 1.5	10.35 ± 1.8	0.70 ± 0.07	20
OL	5.06 ± 1.59	9.24 ± 1.39	0.74 ± 0.07	14
FS	3.04 ± 1.13	7.60 ± 1.53	0.66 ± 0.06	16
RM	0.02 ± 1.05	0.58 ± 1.26	1.03 ± 0.04	88
SS	0.09 ± 1.20	1.25 ± 1.30	0.73 ± 0.08	60

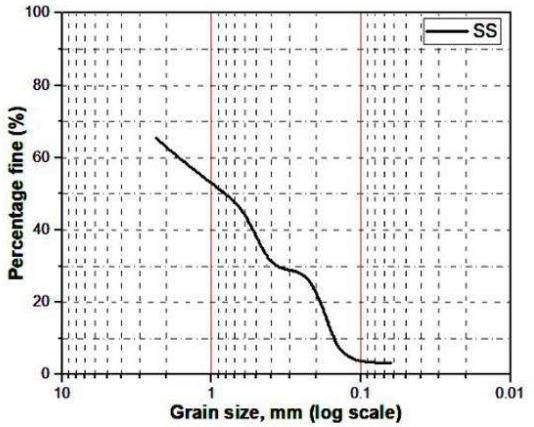
SS
Percentage fine (%)
Grain size, mm (log scale)

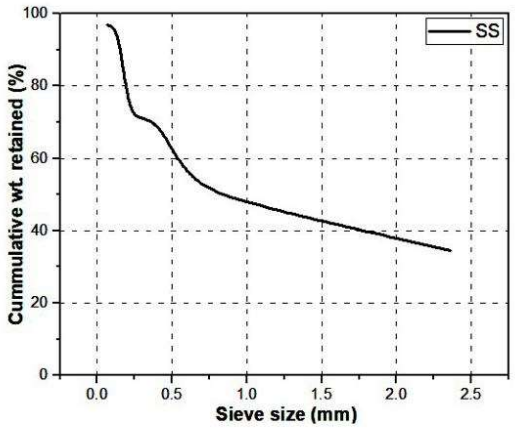
SS
Cummulative wt. retained (%)
Sieve size (mm)

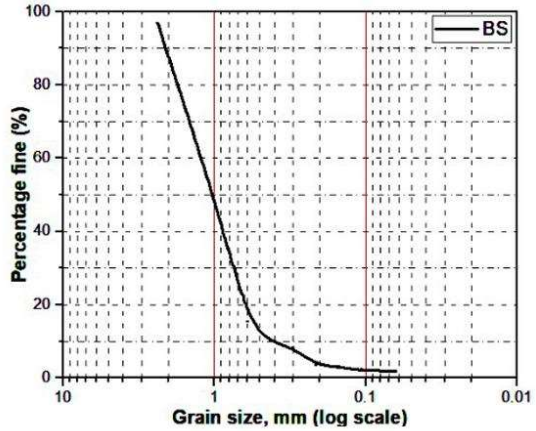
BS
Percentage fine (%)
Grain size, mm (log scale)

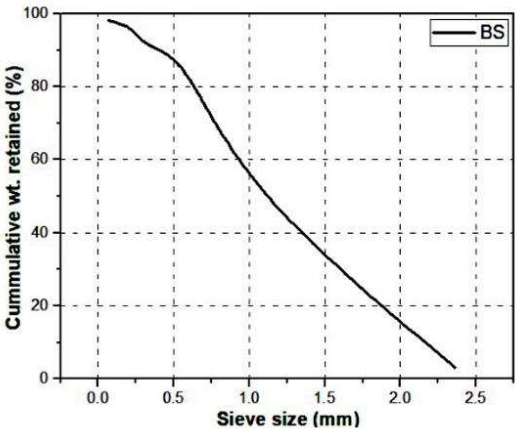
BS
Cummulative wt. retained (%)
Sieve size (mm)

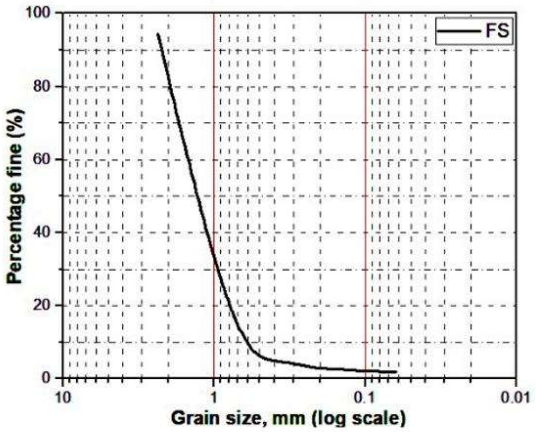
FS
Percentage fine (%)
Grain size, mm (log scale)

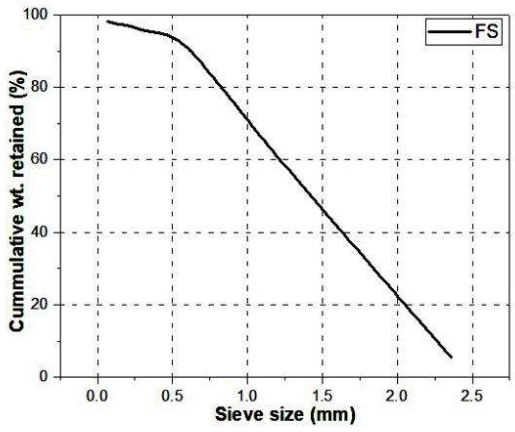
FS
Cummulative wt. retained (%)
Sieve size (mm)

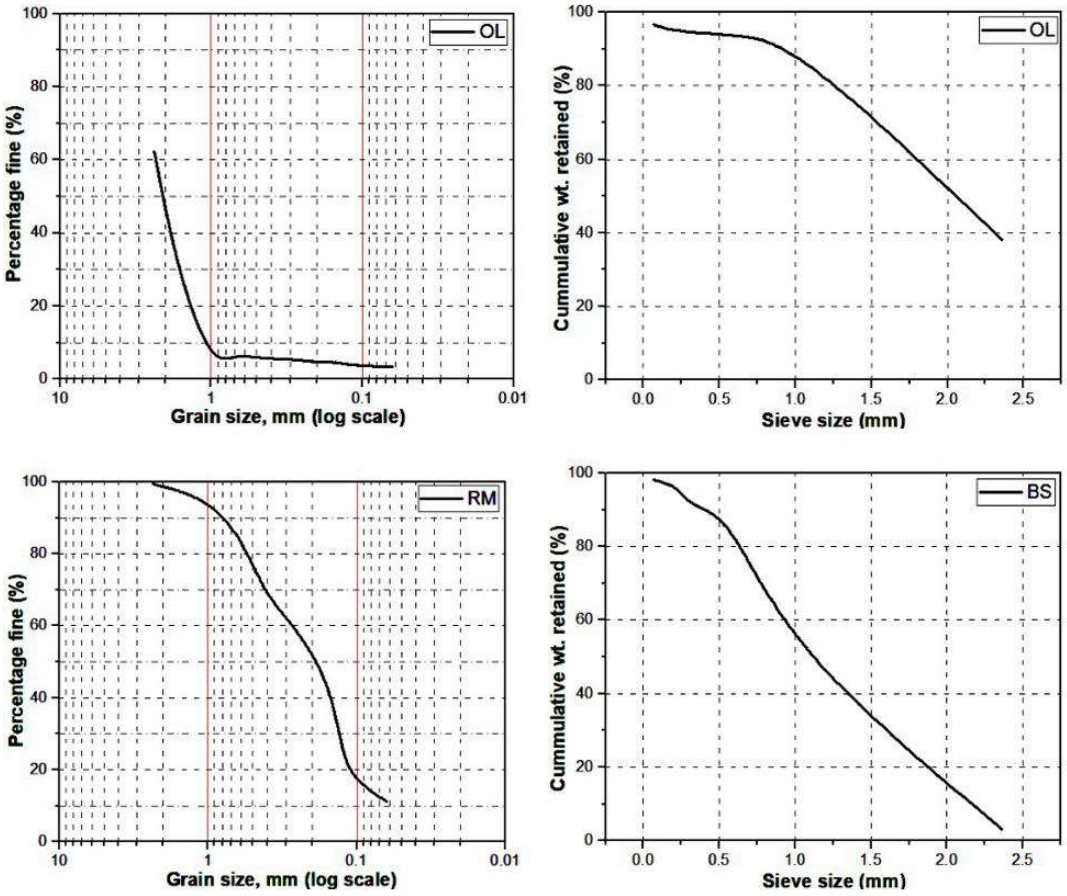

Figure 3.7: Particle size distribution

3.3.6 Clay and moisture content

Figure 3.8 shows the clay content in the different mold materials, it was observed that the maximum and minimum values of clay percentage are 31% and 0.24% present in red mud and ferrochrome slag respectively. Clay present are distinguished by the formation of bonds between the grains by the addition of water and also the formation of bond depends on the hydration of the clay. Red mud has the highest percentage of clay, so it forms better bonding with its grain as compared with the rest. The formation of bonds results in the ideal distribution of thin film around each grain as shown in figure 3.9. The moisture % of SS, BS, and FS has less than 1% whereas RM has 4.11%, which is the highest value among all the materials as listed in table 3.4.

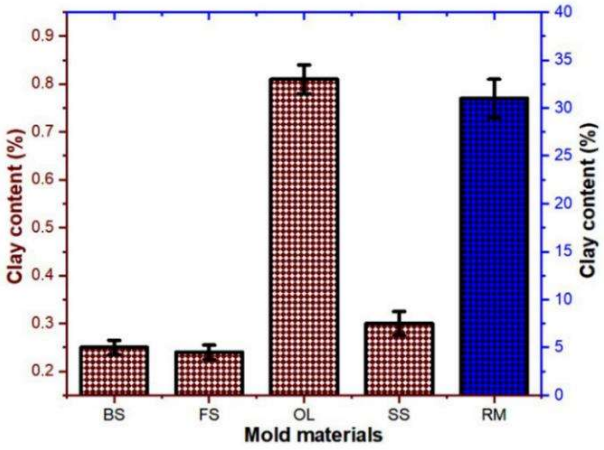

Figure 3.8: Clay content of various mold materials

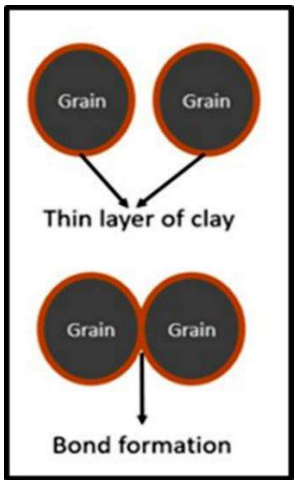

Figure 3.9: Formation of bond between grains

3.3.7 pH value

Table 3.4: pH value and moisture content of materials

Test material	BS	FS	OL	RM	SS
pH	8.13	7.97	8.35	9.94	7.64
Moisture%	0.64	0.33	1.41	4.11	0.75

The pH value of all the materials shows that they are basic having a pH value greater than 7 as listed in table 3.4.

3.3.8 Flowability behaviour

i. *Angle of repose*

Figure 3.10 shows the cone developed during the experiment and figure 3.11 shows the angle of repose of mold materials. The angle of repose for all five materials was observed in the range of 34° – 38°. From table 3.1 the flow behaviour of different materials can be grouped into free-flowing and fair to flow as shown in figure 3.11. Coarse grain showed lower AOR in comparison to fine grain which is supposed to be because of the number of contacts per unit area that is inversely proportional to the square of particle diameters. As the particle size decreases the strength of bulk solid increases and also surface

area increases which enhanced the intermolecular forces that decrease the flowability behaviour of materials. RM has more interparticle interaction in comparison to the remaining particles. So, the flowability behaviour of BS, FS, and OL was quite good as the sand.

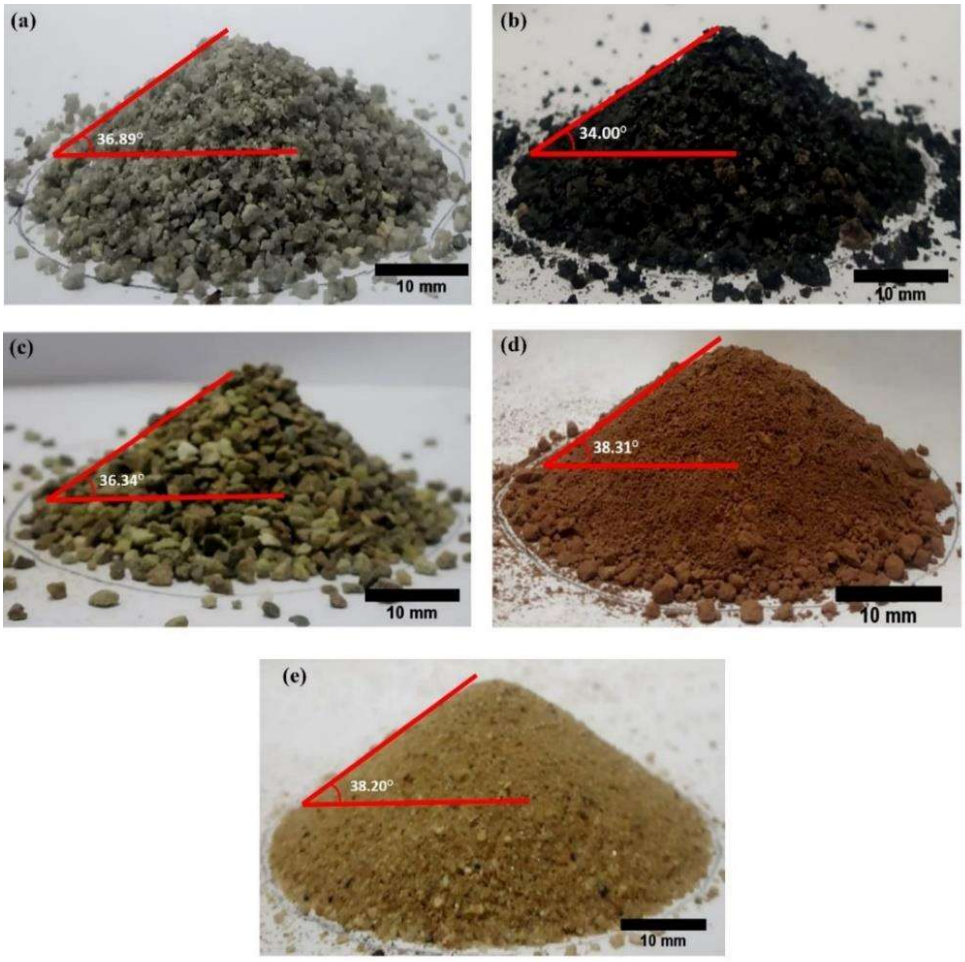

Figure 3.10: Occurrence of cone and static angle of repose of five materials

i. *Hall flow meter test*

Figure 3.12(a) shows the result of the Hall flow test of different materials that represent the volume/mass flow rate of particles. Qualitatively there are trends of decreasing discharge time as per increasing particle size, which improved the flow behaviour. OL shows a high-volume flow rate compared to remaining materials due to having a higher

density. Slag materials showed good flowability as evidenced by high flow rate value as well as silica sand due to low mechanical interlocking between interparticle interactions. The generation of additional frictional resistance between the wall and the particle hindered the flowability behaviour of particles. The results obtained from the angle of repose, Hausner ratio, and Carr index indicated approximately similar flowability behaviour of BS and FS as the sand. However, Hall flow analysis showed higher flowability for OL.

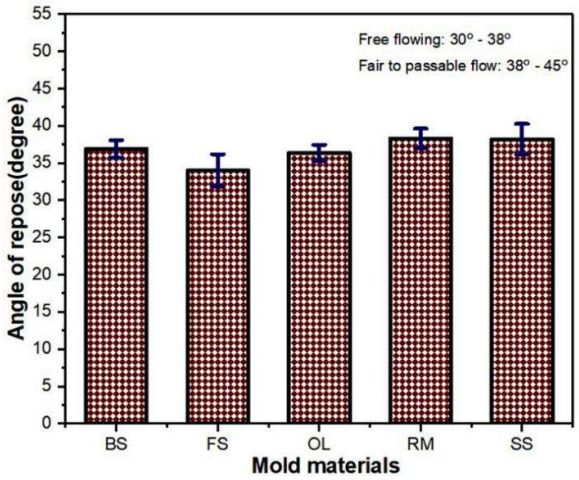

Figure 3.11: Angle of repose and flow behaviour

ii. *Hausner ratio (HR)*

Figure 3.12 (b) shows the result for the Hausner ratio of all five materials. Table 3.5 was developed based on table 3.1. Table 3.5 represent the flow characteristics for all five materials. According to HR values, flow behaviour is characterized as excellent, good, and fair flow. Particle size and shape had a great influence on the Hausner ratio. It had also observed that the aspect ratio of a particle is directly proportional to the angle of internal friction [177]. The smaller the Hausner ratio, the better the flowability. The D50 of BS and FS were 1mm which indicated good flowability behaviour. However, the value for other particles falls in good and fairly flow regions.

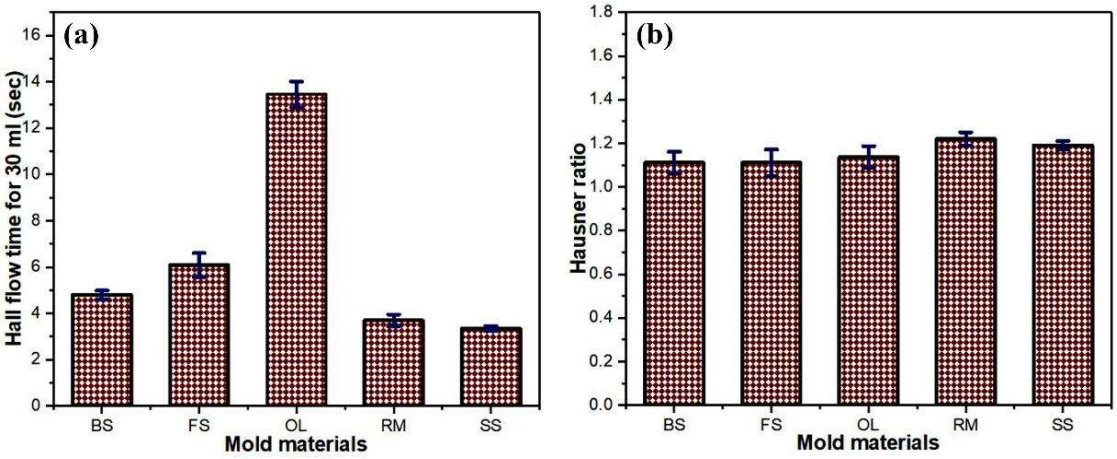

Figure 3.12: (a) Discharge time (b) Hausner ratio with respect to mold materials

Table 3.5: Hausner ratio with flow behaviour

Material	Hausner ratio	Flow behaviour	Carr index	Flow behaviour
BS	1.11 ± 0.05	Excellent	10	Excellent
FS	1.11 ± 0.06	Excellent	10	Excellent
OL	1.13 ± 0.05	Good	12	Good
RM	1.21 ± 0.03	Fair	18	Fair
SS	1.19 ± 0.02	Fair	16	Fair

3.3.9 Relationship between particle shape, particle size distribution, and flow rate

The flowability behaviour for all five materials was based on density, particle shape, and size distribution. A homogenous flow rate of 1mm particle size shows excellent flowability. Also, particles having a wide range of particle size distribution exhibit better flowability. In a wide range of distribution, a small particle will occupy void space created by a coarse particle during flow. There is an optimum range of distribution at which flow behaviour is excellent and beyond that range, flow behaviour will be poor. This was concluded based on the above five materials having different particle shapes and particle size distribution. In a nutshell, specific particle size and particle size distribution are essential for excellent flowability behaviour.

3.4 Conclusions

Following conclusions are drawn-

- Chemical analysis states that SiO_2 is the common phase among the mold materials such as solid waste and sand and the XRD spectrum of mold materials confirms the presence of the SiO_2 phase.
- TGA study states the weight reduction of blast furnace slag, ferrochrome slag, red mud, olivine sand, and silica sand are 4.4%, 3.5%, 10.07%, 12.25%, and 3.1% respectively when heated upto 1000°C.
- GFN of blast furnace slag, ferrochrome slag, red mud, olivine sand, and silica sand are 20,14,16,88 and 60 respectively. Solid waste grains are coarser as compared with sand.
- The grain shape of blast furnace slag, ferrochrome slag, olivine sand, and silica sand particles are similar due to having approximately the same HSC value but a red mud grain shape spherical with an HSC value of 1.
- pH study states the mold material used in the present investigation is basic in nature.
- The flowability behaviour of solid waste is quite good as silica sand.